Carpathian Journal of Earth and Environmental Sciences August 2023, Vol. 18, No. 2, p. 231 – 244; DOI:10.26471/cjees/2023/018/254

INTERPRETATION OF THE MAGMA CHAMBER PROCESSES USING MICRO-TEXTURE AND ZONING STYLES IN PLAGIOCLASE CRYSTALS: EVIDENCE FROM THE ANDESITIC ROCKS IN SABZEVAR ZONE (NE IRAN)

Soheila SAKI[1], Papadopoulou LAMBRINI[2], Amir Ali TABBAKH SHABANI[3]*, Mahmoud SADEGHIAN[4], Mehdi REZAEI KAHKHAEI[5], & Morteza DELAVARI KOSHAN[6]

[1,3,6] Faculty of Earth Sciences, Kharazmi University, Tehran, Iran aatshabani@khu.ac.ir
[2]School of Geology, Aristotle University of Thessaloniki, Greece
[4,5]Department of Petrology and Economic Geology, Faculty of Earth Sciences, Shahrood University of Technology, Shahrood, Iran

Abstract: Investigation of variations in the micro-texture and chemical composition of plagioclases (core to rim) allows the sequencing of the magma chamber processes and helps interprete and associate textures to specific processes. In this contribution, the micro-textures and chemical zoning of the plagioclases, significant recorder of magma chamber processes, from the west of Torbat-e-Heydariyeh andesitic rocks (WTHAR) are considered to decipher the physical and chemical parameters of magma evolution. The rocks are cropped out in the northern branch of Neotethyan magmatic belt and considered as the products of Eocene magmatic activities of the Sabzevar zone (N-NE Iran). The rocks show vitrorphyric and vitroglomeroporphyric textures with main phenocrysts, plagioclase (andesine, labradorite, and bytownite), clinopyroxene (augite), orthopyroxene and magnetite scattered in a glassy matrix. The recognized micro-textures of the WTHA plagioclases can be divided into two categories: (i) growth- related textures in the form of coarse-sieved (CS), fine-sieved (FS), core sieved and intact margin (CSIM), core intact and sieved margin (CISM) and entirely sieved (ES) morphologies, oscillatory zoning (OZ), rounded zone corner (RZC) and resorption surfaces (RS) formed due to the changes in temperature, melt H_2O content, pressure, composition of the melt, equilibrium at the crystal-melt interface and (ii) morphological textures such as glomerocrysts (GLO), synneusis (SY), swallow-tail (ST) crystals, broken crystals (BC), formed by the effect of dynamic behavior of the crystallizing magma (convection, degassing, etc.) and magmatic differentiation. Also, the occurrence of these changes can be related to the self-mixing process in the magma chamber. The self-mixing with recharge event can be the reason for the dynamic activities in the magma chamber.

Key words: magma chamber, plagioclase, micro-textures, zoning, andesite, Sabzevar zone, Iran

1. INTRODUCTION

The study of chemical changes in calc-alkaline magmatic rocks related to a subduction zone is very important because these changes are the result of factors such as crystal separation, digestion, magma mixing, or contamination (Lindh et al., 2006). Plagioclase commonly shows a variety of disequilibrium textures in volcanic rocks, particularly in andesites (Nelson & Montana, 1992). The mineral assemblages and mineral chemistry are related to the composition of the host magma and the physico-chemical conditions of the melt during crystallization (Helmy et al., 2004; Molina et al., 2009; Yousefi et al., 2017 a). Therefore, the evaluation of crystallization conditions and the processes influencing mineral crystallization could explain the magmatic evolution of the host rocks accurately. (Mobashergarmi et al., 2018). As minerals can be highly susceptible to modifications in the magmatic system and able to record the changes in thermodynamic equilibria in their compositional zoning patterns, resorption and dissolution textures are commonly utilized to define the magma chamber processes (Korkmaz & Kurt, 2021). In particular, texture and chemical zoning in plagioclase

may be a powerful tool for the identification of the dynamics and kinetics of the magmatic process, due to being an abundant phase in lavas from a wide range of geotectonic settings (Bennett et al., 2019; Nelson & Montana, 1992; Renjith, 2014). The evolution of magma chamber processes is of major petrologic interest and has been studied widely (Hoshide & Obata, 2009). This study presents various textures in plagioclase of the WTHAR (NE Iran) for the first time and based on their various textures, their growth history is interpreted carefully. These andesitic rocks have not been subjected to detailed studies of mineral chemistry and magma chamber processes, therefore, a detailed and systematic approach of the evaluation of crystallization conditions is necessary. The results of this article provide useful information on the sequence of events and temporal change of physico-chemical conditions in the magmatic system. After a geological outline, petrography and whole-rock geochemistry, analytical data on plagioclase texture and zoning are presented, showing that the textures and zoning patterns correlate well with host rock types, providing good information on the evolution of magma chamber processes.

2. GEOLOGICAL SETTING

Igneous activity in Iran commenced in the early Paleocene, and is still continuing to the present (e.g., Alaminia et al., 2013; Pang et al., 2013; Ghasemi & Rezaei, 2015; Shafaii Moghadam et al., 2015, 2016; Alizadeh et al., 2017; Almasi et al., 2019; Kazemi et al., 2019; Sepidbar et al., 2021; Shahbazi et al., 2021). It is manifested in the form of a triangular loop around the Central Iran structural zone, including the Urumieh Dokhtar magmatic belt in the northwest-southeast, Alborz zone in the north, which continues to the study area, the west of Torbat-e-Heydariyeh and Lut block in the east (Figure. 1). Cenozoic extensive magmatism is irregularly distributed throughout Central Iran. The most intense magmatic activity in the early Tertiary, especially in the Eocene, occurred in two forms (volcanism and plutonism). The magmatic activities of the Miocene, or to be more precise, the late Miocene to the present , are mainly volcanic and have basaltic and andesitic composition. In Iran, they have scattered outcrops, are less widespread. It seems that most of this group of volcanic activities were formed in tectonic environments within the continent and often erupted or flowed in dry or shallow water environments such as lakes. This group of magmatic activities are often attributed to the Quaternary, but field and stratigraphic evidence contradicts this.

The Cenozoic magmatic events associated with the closure of the Neo-Tethys were important in depicting the face of present-day Iran. There are two prominent stages of magmatic activity during the Cenozoic, especially in the Eocene and Plio-Quaternary (Yousefi et al., 2017 b). The volcanic activity culminated in the Middle–Upper Eocene and continued in the Neogene and Quaternary (Ghasemi &

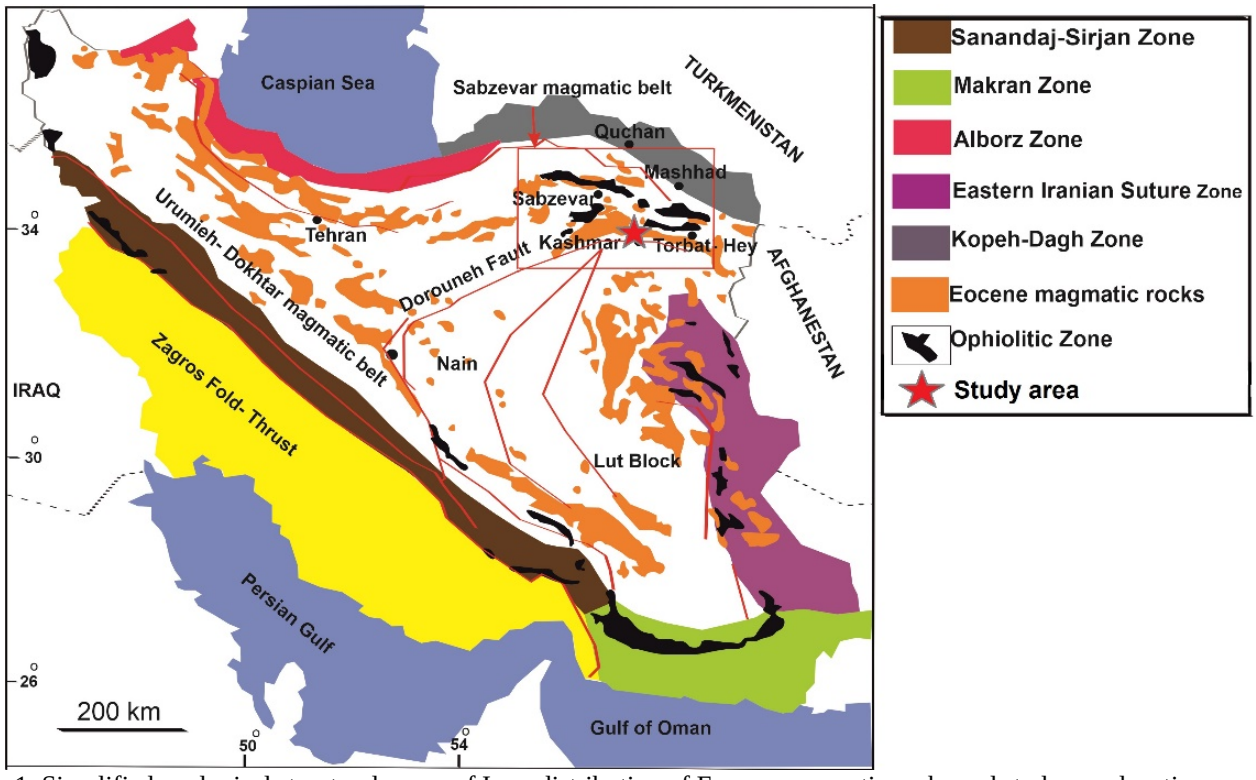

Figure 1. Simplified geological structural zones of Iran, distribution of Eocene magmatic rocks and study area location (modified after Shafaii Moghadam et al., 2015).

Rezaei Kahkhaei, 2015; Yousefi et al., 2017 b). The subduction of Sabzevar (opened in the Late Triassic-Early Jurassic and closed at the Late Cretaceous, (Baluchi, 2019; Kazemi et al., 2019) Oceanic lithosphere (eastern branch of Neotethys) controls volcanic activities in northeastern and central Iran. Major fault systems such as the Doruneh Fault have played an important role in the generation and emplacement of the magmas in this zone (Berberian & King, 1981). At the west and northwest of the Torbat-e-Heydariyeh area, a small part of the Sabzevar zone occurs which extends to the west of Torbat-e-Heydariyeh city in Khorasan Razavi province (NE Iran). This zone is a large magmatic belt developed during the early Paleocene to Plio-Quaternary (Shafaii Moghadam et al., 2015) along the northern edge of Central Iran and the southern margin of Alborz (Figure 1). The Torbat-e-Heydariyeh andesitic rocks overlie the Paleocene-Eocene pyroclastic rocks and have Middle Eocene age.

3. MATERIALS AND ANALYTICAL METHODS

The rocks are characterized by their dark grey color in outcrop, but black on fresh surfaces. Columnar jointing is a characteristic cooling feature of this eruptive unit (Figure 2). According to field evidence and petrographic research, the studied samples are very similar to basaltic rocks due to their dark color and and columnar joints. One hundred samples were collected from the volcanic rocks of Torbat-e-Heydarieh area and then 90 thin sections were prepared.

3.1. Whole-rock geochemistry

Twenty andesite samples were selected for whole-rock analyses. Whole-rock major and trace elements were analyzed by X-Ray Fluorescence Spectrometry (XRF, Primus II, Rigaku) and Agilent 7700e ICP-MS at the Wuhan sample solution analytical laboratory Co., Ltd., Wuhan, China. Details of the analytical method and geochemical compositions of the samples are presented in supplementary files.

3.2. Mineral-chemical analysis

We selected six fresh samples of andesitic rocks for microanalysis. Mineral compositions were determined by a scanning electron microscope (JEOL JSM-6390LV) equipped with an energy dispersive spectrometer (EDS) (INCA 300, Oxford) with 20kV accelerating voltage and 0.4mA probe current and a wavelength dispersive spectrometer (WDS) (INCAWave, Oxford) at the Laboratory of Electron Microscopy, Aristotle University of Thessaloniki, Greece. The results of plagioclase analysis are presented in Table 1.

4. RESULTS

4.1. Petrography and micro-textures in plagioclase

In order to determine their textures, mineral contents and rock types. Clinopyroxene, orthopyroxene, plagioclase and opaque minerals are recognized as microphenocrysts (Figure 3). These microphenocrysts are fresh and almost euhedral to subhedral scattered in a glassy groundmass; therefore, vitrophyric and vitro-glomerophyric are considered as the main textural types (Figure 3). Micro-textures of plagioclases in the study area are presented in Table 2 and Figure 4.

4.2. Whole-rock geochemistry

Geochemically, the samples exhibit a narrow range of values for SiO_2 (59.95–61.45 wt%), Fe_2O_3(t)

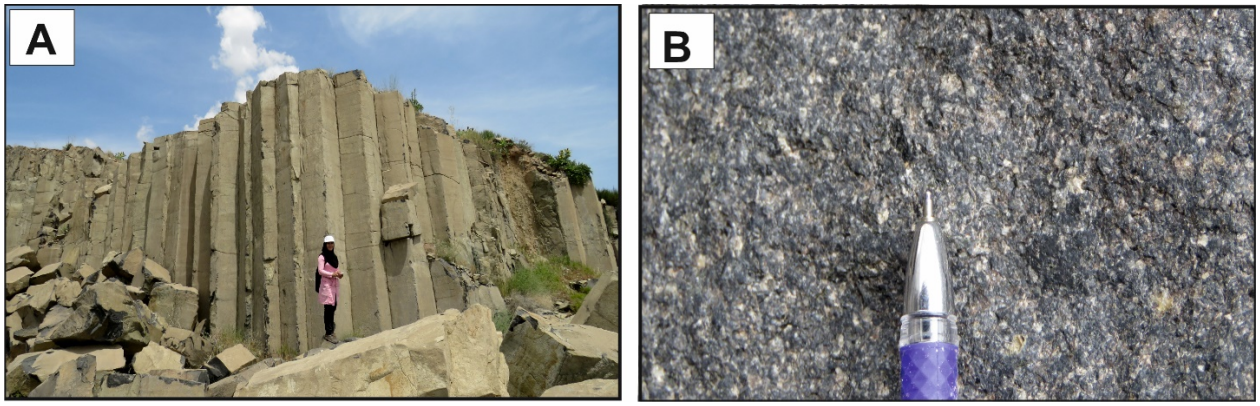

Figure 2. A) Field photograph of spectacular columnar joints of andesitic rock in quarry in the western part of Torbat-e-Heydarieh (X:680720; Y: 3917833); B) close view of the andesitic sample.

Table 1 Results of some analysis of core to rim compositional profiles of plagioclase in WTHAR.

Sample	Location	SiO_2	Al_2O_3	FeO	MgO	CaO	Na_2O	K_2O	Or (K)	Ab (Na)	An (Ca+Mn+Mg)
ST5-2C1	Rim	46.34	34.13	0.67	0.04	17.65	1.38	0.04	0.24	12.34	87.42
		47.37	33.50	0.33	0.00	16.49	1.93	0.23	1.35	17.22	81.43
		46.92	33.84	0.51	0.00	17.48	1.45	0.18	1.08	12.87	86.05
		46.40	33.72	0.82	0.15	17.05	1.65	0.00	0.00	14.77	85.23
	Core	48.35	32.99	0.43	0.18	15.61	2.52	0.04	0.24	22.28	77.48
		54.16	28.78	0.57	0.12	11.48	4.72	0.39	2.25	41.34	56.41
		47.10	33.82	0.11	0.07	16.57	1.82	0.23	1.35	16.29	82.36
	Rim	49.07	31.78	0.67	0.00	15.06	2.83	0.17	1.01	25.12	73.88
ST1-5	Rim	53.82	28.40	0.79	0.00	11.12	4.47	0.94	5.49	39.67	54.47
		56.00	27.64	0.42	0.00	9.74	5.62	0.72	4.11	48.94	46.89
		50.30	31.59	0.30	0.00	14.24	3.30	0.19	1.10	29.15	69.49
		54.10	28.50	0.66	0.21	10.71	4.84	0.71	4.11	42.47	53.27
	Core	53.72	29.07	0.34	0.06	11.52	4.68	0.47	2.70	41.08	56.22
		55.54	28.11	0.23	0.00	10.15	5.48	0.61	3.51	47.71	48.78
		50.96	31.10	0.44	0.12	13.58	3.75	0.00	0.00	32.95	66.70
		53.90	28.41	0.67	0.02	11.03	4.82	0.60	3.49	42.54	53.97
	Rim	53.84	28.47	0.94	0.37	10.97	4.43	0.92	5.33	38.80	55.67
ST3-2	Rim	48.44	32.29	0.58	0.14	15.69	2.31	0.21	1.22	20.61	78.17
		48.27	31.83	0.14	0.36	14.70	2.54	0.18	1.06	22.98	75.95
		48.77	32.54	0.61	0.29	15.37	2.55	0.02	0.12	22.59	77.28
	Core	48.91	32.68	0.31	0.15	15.16	2.75	0.12	0.67	24.30	75.03
		49.05	32.75	0.34	0.00	15.63	2.49	0.28	1.66	22.00	76.34
	Rim	47.95	32.68	0.55	0.18	16.16	2.08	0.05	0.32	18.59	81.09
ST5-2-C2	Rim	54.54	28.24	0.77	0.17	10.87	4.68	0.80	5.00	41.09	53.92
		49.51	32.33	0.17	0.20	14.75	2.92	0.12	0.69	25.86	73.46
		50.84	31.54	0.11	0.00	14.22	3.55	0.00	0.00	31.10	68.90
	Core	48.90	32.18	0.98	0.22	15.07	2.64	0.23	1.33	23.40	75.27
		50.96	30.80	0.42	-0.03	13.84	3.34	0.49	2.88	29.59	67.52
	Rim	49.42	31.85	0.83	0.45	14.72	2.53	0.50	2.90	22.33	74.77

(6.25–7.94 wt%), Na_2O (3.21–3.66 wt%), K_2O (1.24–2.76 wt%), Al_2O_3 (15.33–15.73 wt%), and Mg# (51.3–55.1). MnO, P_2O_5, and TiO_2 are <1 wt%. All the studied rocks are located in the andesite compositional domain on the TAS diagram (Figure 5a) (Le Bas et al., 1986), and also plot in the medium to high-K calc-alkaline fields of Gill (1981) diagram (Figure 5b). The primitive mantle-normalized spider diagram (Sun & McDonough, 1989; Figure 6) shows significant negative anomalies of HFSE (high field strength elements) such as Ti, Nb and P, and positive anomalies of large ion lithophile elements (LILE), such as K, Cs, U and Rb. The patterns exhibit similar distribution to volcanic arc (Figure 7) rocks (Yan et al., 2019; Zhang et al., 2019; Sivell & Waterhouse, 1988), typical convergent margin and subduction setting.

4.3. Mineral chemistry

The most abundant phenocrysts in WTHA rocks are plagioclase characterized in most cases by sieve texture (Figure 4), and oscillatory zoning (Figures 4F and E). The compositional spectrum of plagioclase in this suite ranges from andesine to bytownite (Figure 8; Deer et al., 1992); i.e, their An contents vary from 44.3 to 85.1.

5. DISCUSSION

5.1. Interpretation of micro-textures

5.1.1. Sieve textures

The composition of magmatic plagioclases depends upon physicochemical parameters such as temperature (T), total pressure (P) and water content of the melt (wt% H_2O). Changes in these intensive parameters lead to the formation of different micro-textures (Renjith, 2014). Sieve texture in plagioclase is one of the most prominent in the microscopic thin sections of WTHA rocks. It is a non-equilibrium texture and is formed following the physical and chemical changes in the magma chamber (Shelley, 1993). Therefore, careful examination can reveal information concerning the conditions governing the magma chamber. The sieve texture in coarse and fine sizes is a result of glass and iron oxide inclusions, which gives a spongy appearance to the crystals. The size of the sieves can depend on the increase of magma ascent speed or the increase in magma water content during ascent (Viccaro et al., 2010). The relationship and size of the sieves indicate severe or long-term dissolution.

There are two main causes for the formation of sieve textures: 1- pressure reduction (Nelson &

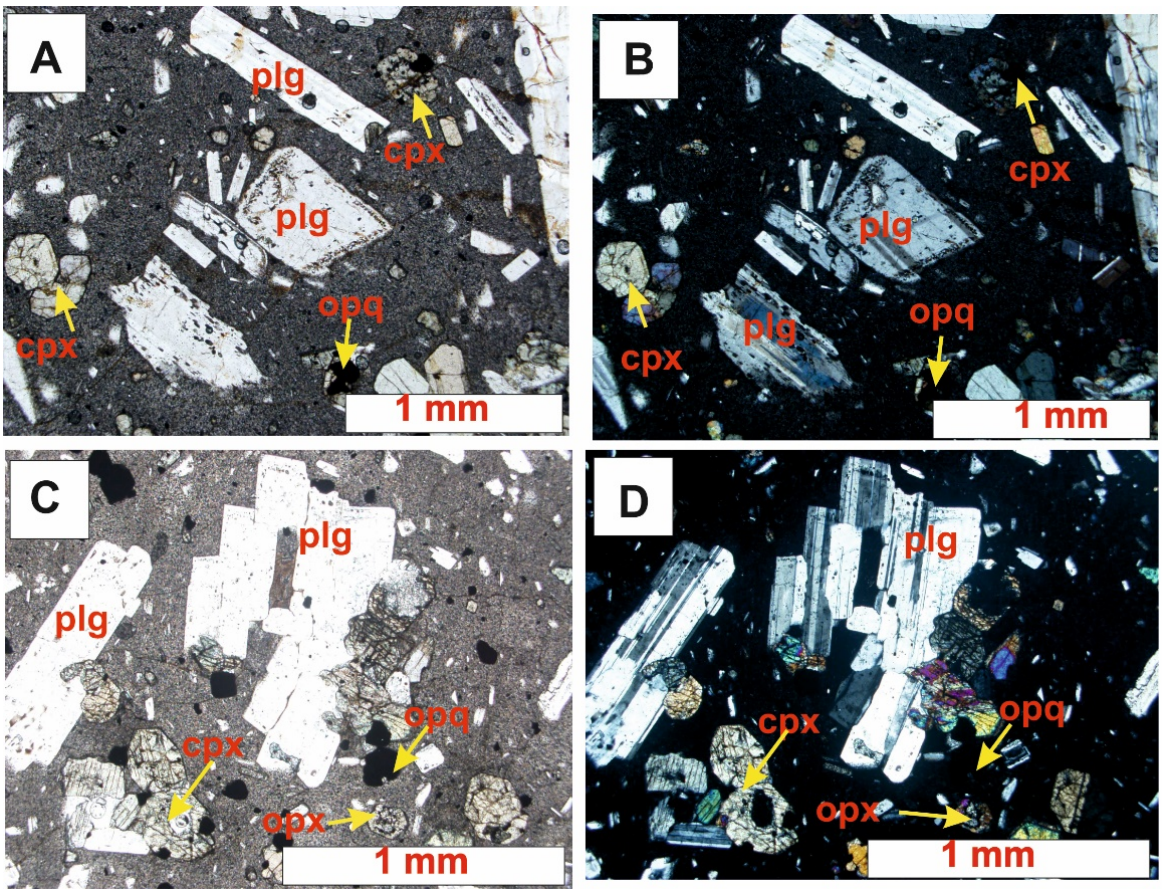

Figure 3. Photomicrographs of WTHA samples with variable euhedral to subhedral phenocrysts of plagioclase, clinopyroxene, orthopyroxene and opaque minerals, and rare orthopyroxene in a quenched groundmass. A, B) Vitrophyric and C, D) vitro-glomerophyric textures. (A,C: PPL; B, D: XPL).
Abbreviations: plg: plagioclase; cpx: clinopyroxene; opx: orthopyroxene; opq: opaque.

Montana, 1992; Shelley, 1993), 2- magma mixing, reaction with hotter Ca-rich melt (Tsuchiyama, 1985). In the first case, during decompression, when a H_2O undersaturated magma rises fast, the $P_{(H2O)}$ of the system increases, therefore, reducing the stability of plagioclase and crystal dissolution occurs (Nelson & Montana, 1992). Plagioclase crystals become unstable during ascent and melt partially. Depending on whether the temperature drop is fast or slow, these partial melts crystallize in the form of glass or new plagioclase crystal and lead to the creation of a sieve texture (Blundy & Cashman, 2005; Renjith, 2014; Jamshidibadr et al., 2020). The coarse-sieve micro-texture is the result of this process (Nelson & Montana 1992).

In the second case, plagioclase crystals tolerate dissolution when magma interacts with a hotter Ca-rich magma (Tsuchiyama, 1985). The fine-sieve micro-textures are produced by this process. The sieve textures are usually interpreted as resulting from magma mixing, but they may also occur by rapid decompression, where heat loss is minor relative to the ascent rate (Nelson & Montana, 1992).

Coarse-sieve (CS) texture is seen in different forms in the studied plagioclases (Figure 4). In general, cavities in the CS micro-texture can be divided into two categories, separate sieves and those connected to each other.

In the first category, CS cavities do not follow a specific pattern and occur in the core of the crystal. In the second category two forms are noticed:

A) Elongated and parallel to the plagioclase cleavages. In this case, the cavities or pores intersect and connect.

B) The CS forms a ring in the core of the crystal, with the cavities connected to each other.

Plagioclase sieve cores may be produced by rapid decompression and degassing of plagioclase-saturated magma rising from deep to shallow depth (Landi et al., 2004). The mineral chemistry of WTHA with CS texture ranges between labradorite and bytownite. The trend of plagioclase An% composition from rim-to-rim shows oscillatory zoning (Figure 9). This variation in the chemistry of plagioclase demonstrates the changes in the chemical composition of magma during crystallization. According to Renijith (2014), absence of growth zoning shows that the phenocryst's cores have grown in a static equilibrium magmatic environment followed by an ascent related

decompression driven dissolution.

The fine-sieve (FS) texture consists of very small inclusions made of glass, giving the crystal a dusty appearance.

They are mainly found in the core and margins of small to medium grains or in the margins of large plagioclase crystals.

Table 2. Different types of plagioclase micro-textures in WTHA. Schematic representation of the illustrated microstructures considered and their interpretations presented in the text.

Texture	Description (abbreviation)	Figure(s)	Relative frequency + (rare), ++ (moderate), +++ (frequent)
	Coarse-sieve (CS): 1-separate sieves 2-connected sieves	4 a, c, d, g, h	+++
	Fine-sieve (FS): entirely sieved (ES) intact core and sieved margin (CISM) sieved core an intact margins (CSIM)	4 a, b, c, d, g, h	+++
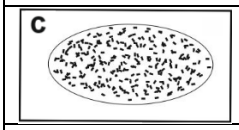	Core sieved and intact margin (CSIM)	4a, c	++
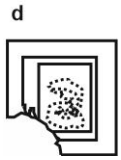	Broken crystal (BC)	4b, d, e, h	+
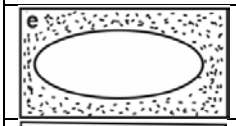	Core intact and sieved margin (CISM)	4d	++
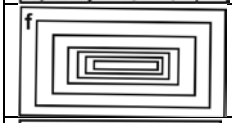	Oscillatory zoning (OZ)	4e, f	++
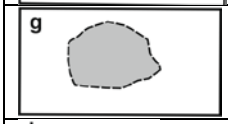	Resorption surface (RS)	4b, d, h	+++
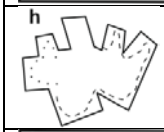	Glomerocrysts (GLO)	4g	++
	Rounded zone corner (RZC)	4i	+
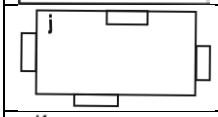	Synneusis morphology (SY)	4i, 4a, b, h	++
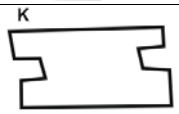	Swallow-tail (ST)	4b, h	+
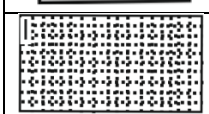	Entirely sieve (ES)	4h	+++
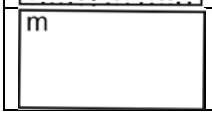	Intact crystals (IC)	4j, 4c, g	+++

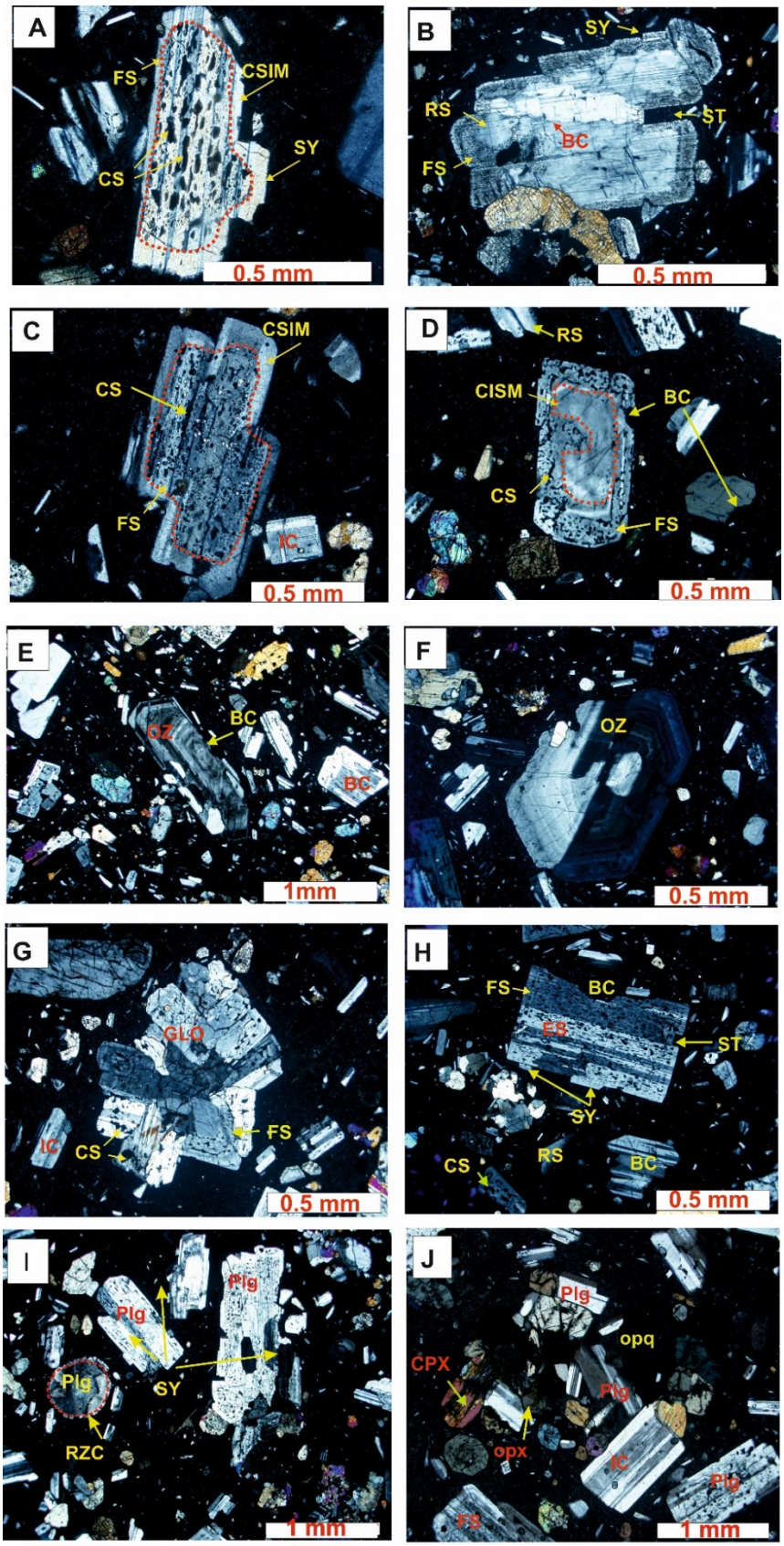

Figure 4. Photomicrographs of plagioclase micro-textures (in XPL) Abbreviations are given in Figure 3 and Table 2.

Types of observed FS in the studied samples:

A: Plagioclase crystals that are entirely sieved (ES)

This texture can be due to the uniform composition of the plagioclase that with changing conditions, the whole crystal begins to corrode (Shelley, 1993).

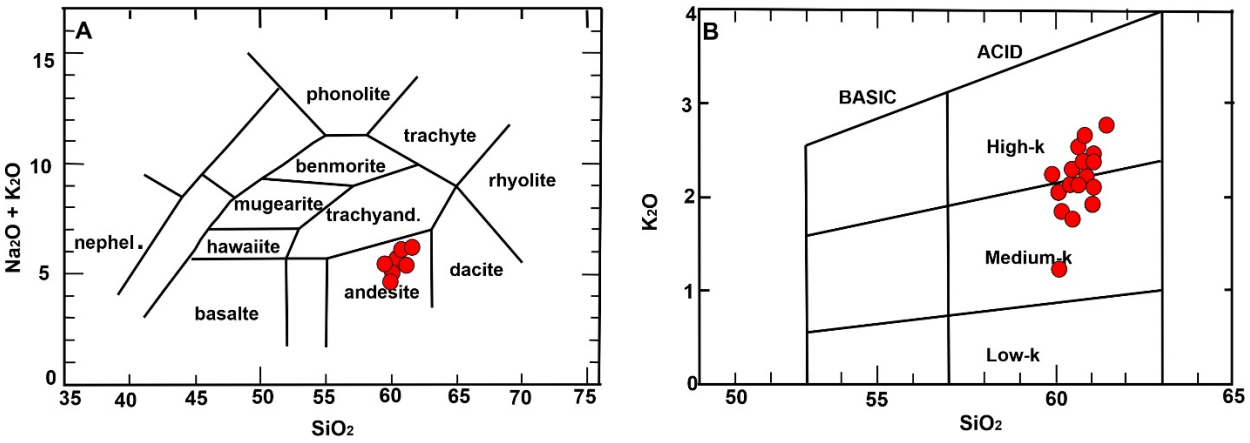

Figure 5. A) Classification of WTHA volcanic rocks on Le Bas et al., (1986); B) Gill (1981)) diagrams showing medium to high-K calc-alkaline series.

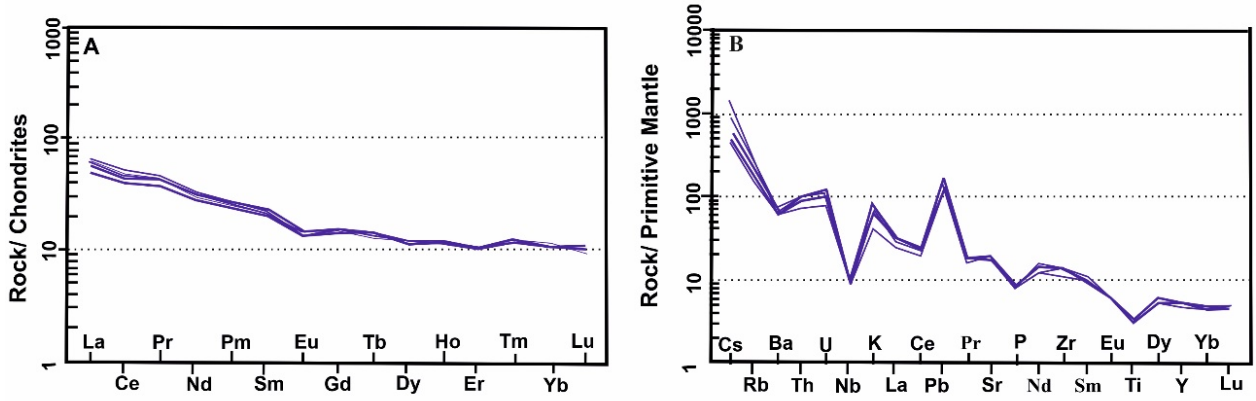

Figure 6. A) Chondrite-normalized REE diagram for the THA, B) Primitive Mantle normalized multi-element patterns. Normalizing values are from Sun and McDonough (1989).

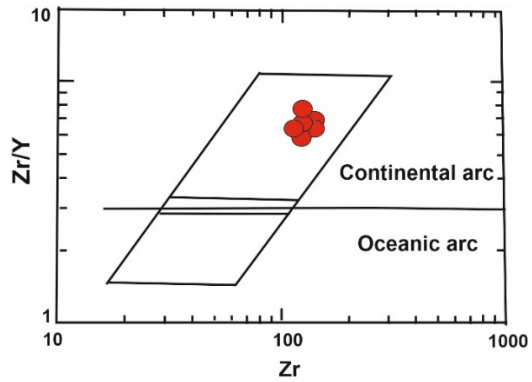

Figure 7. Plot of the studied samples on tectonic discrimination diagram Zr/Y versus Zr (ppm) (Pearce, 1983).

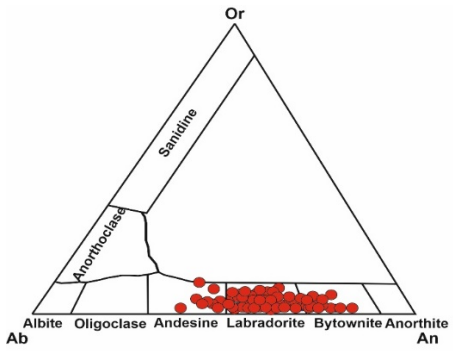

Figure 8. Plot of plagioclase analyses on Ab-An-Or ternary diagram from Deer et al. (1992).

B: Plagioclase crystals, with an intact core surrounded by a sieved margin (CISM).

Shelley (1993) believes that in many cases, in the core of plagioclase phenocrysts, a sieve ring of plagioclase grows that has a higher calcium content than the nucleus of these crystals. The existence of unbalanced conditions is the main cause of the creation of these rings, which are formed by rapid growth due to mixing with a hotter magma richer in H_2O and Ca (Tsuchiyama, 1985).

C: Plagioclase crystals with a sieved core but intact margins (CSIM).

This form of sieve texture may occur under H_2O-saturated conditions following a sudden pressure drop during magma ascent from depth to the surface (Nielson & Montana, 1992; Renijith, 2013).

The FS micro-textures occur in the core, rim or even in entire crystals as observed in WTHAR. Mineral chemistry of the plagioclases with FS texture ranges from andesine to labradorite. Rim-to-rim trend

of anorthite content shows oscillatory zoning (Figure 10). In some samples An% content increases from core to rim. This variation depicts changes in the chemical composition of magma during crystallization, which caused the formation of FS micro-texture. In the studied plagioclases, FS micro-texture is formed by increase of magma temperature and partial melting. Finally, we can briefly conclude that FS in the samples seems to be developed when the plagioclases have undergone partial dissolution by interacting with a hotter Ca-rich melt.

5.1.2. Resorption surface (RS)

As seen in Figure 4b, d, h, and Table 2g resorption surfaces (RS) are observed in many of the studied plagioclase crystals. RS can occur through multiple processes such as a change in the composition of the system and magma mixing. The processe(s) must occur repetitively to explain the presence of multiple resorption interfaces within individual plagioclases (Bennett et al., 2019).

In the plagioclases of WTHAR, magma mixing could occur multiple times within the system based on changes in Ab% and An% in the RS section (Figure 11).

5.1.3. Rounded zone corner (RZC)

The rounded zone corner (RZC) (Table 2, Figure 4i) is another micro-texture seen in some plagioclase crystals. According to Ginibre et al., (2002a) this phenomenon indicates that during their growth dissolution has occurred.

Due to the heating of plagioclase at a temperature higher than its freezing temperature or due to factors such as magma recharging (Davidson & Tepley (1997), the crystals undergo a process of dissolution and melting.

5.1.4. Synneusis texture (SY)

The synneusis texture (SY) is observed in the rim of some plagioclase crystals of WTHA rocks (Figures 4a, b, and h). Synneusis formation needs a mechanism like shear flow or turbulent mixing to rotate the crystals into alignment (Schwindinger, 1999). This micro-

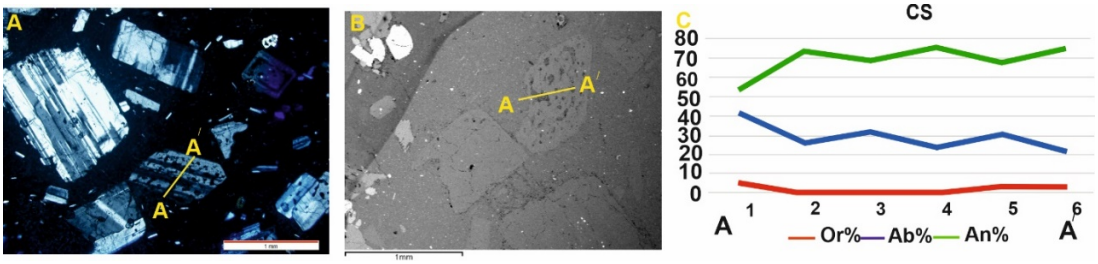

Figure 9. A) Plagioclase with CS micro-textures in XPL; B) BSE image; C) Rim-to-rim profiles of An, Ab, Or % in WTHA rocks.

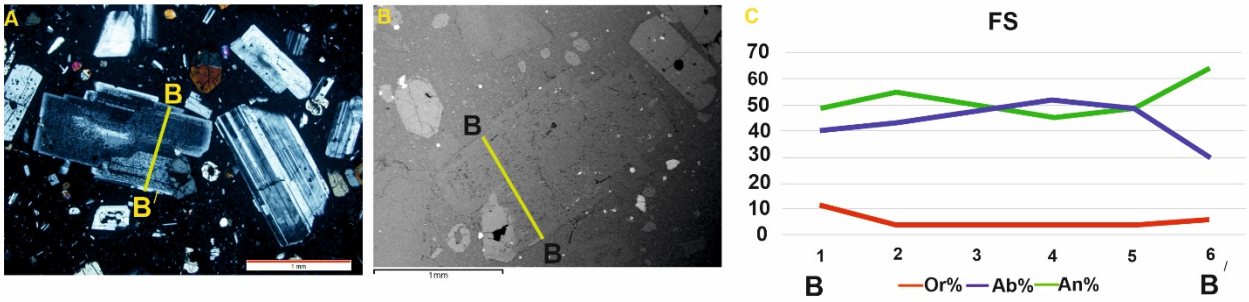

Figure 10. A) Plagioclase with FS micro-textures in XPL; B) BSE image; C) Rim-to-rim profiles of An, Ab, Or %.

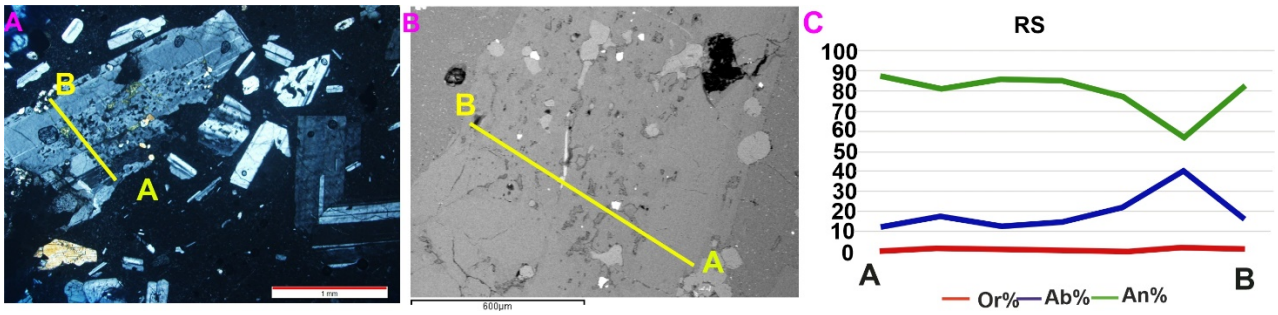

Figure 11. A) Plagioclase with RS micro-textures in XPL; B) BSE image; C) Rim-to-rim profiles of An, Ab, Or %.

texture formed in the magma chamber before crystallization due to the motion of crystals in a liquid-rich magma (Renjith, 2014; Jamshidibadr et al., 2019).

5.1.5. Zoning

Zoning patterns are one of the most spectacular features in crystals, consisting of fine concentric zones of contrasting compositions. Zoning in plagioclase occurs in two forms (Browne et al., 2006):

(i) Repeated changes in the crystallization conditions within crystal growth in a convecting magma chamber.

(ii) Repeated magma refill took after compositional changes, in the event that mechanical and chemical mixing is enough.

In normal zoning, plagioclase cores are relatively enriched in Ca, and outer zones are progressively becoming richer in Na. Reverse zoning indicates disequilibrium conditions that can be caused by a volcanic eruption, rapid movement of magma in a chamber or conduit, rapid release of volatiles in a water-saturated magma, or magma mixing.

Oscillatory zoning in plagioclase, involving alternating calcic and sodic zones with small compositional differences, has been explained by diffusion-controlled, recurrent supersaturation of the melt in anorthite and then albite components adjacent to the growing crystal (Vernon, 2004).

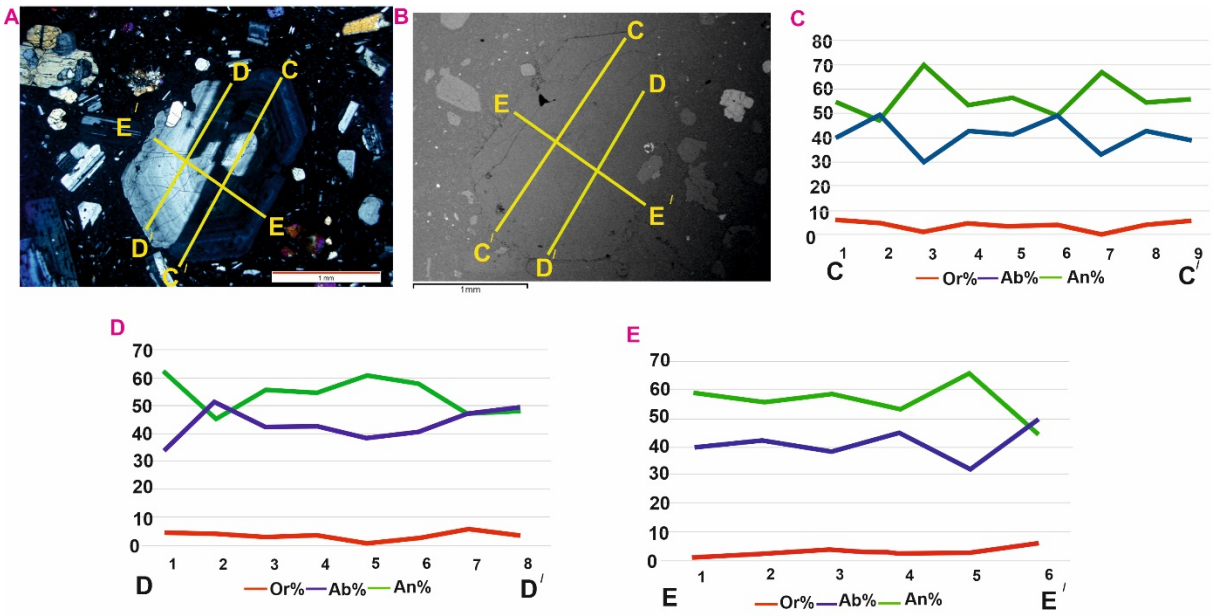

Figure 12. A) Plagioclase with oscillatory zoning in XPL; B) BSE image; C, D and E) Rim-to-rim profiles of An, Ab, Or %.

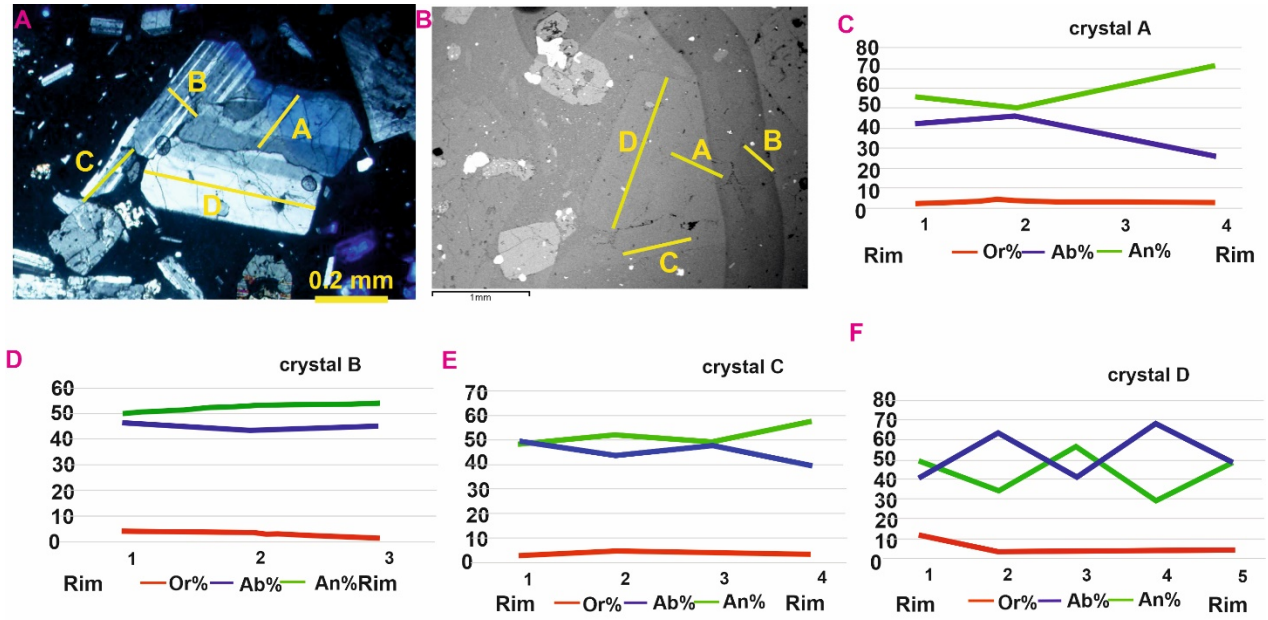

Figure 13. A) Plagioclase with glomerocrystic texture in XPL; B) BSE image; C, D, E and F) Rim-to-rim profiles of An, Ab, Or % from phenocrysts 1, 2, 3 and 4.

Normal, reverse and oscillatory zoning (small- and large-scale oscillations) have been observed in plagioclases of WTHA rocks. In normal zoning of the plagioclases, from core to rim, the amount of anorthite decreases. In reverse zoning, plagioclase cores have an andesine composition and their margins have a labradorite composition, i.e., the amount of anorthite increases from core to rim. In the studied samples most of the crystals have oscillatory zoning (Figure 12). As seen in Figure 10c, d, e the number of anorthite changes from core to rim in an oscillatory manner.

5.1.6. Glomerocrysts (GLO)

Glomerocrysts are the aggregates of two or more plagioclase phenocrysts formed when the partially resorbed crystals get spatially closer (Renjith, 2014). The association of CS and FS with glomerocrysts in the studied samples suggest that before they get sutured phenocrysts have undergone partial dissolution (Figure 4g).

According to the chemical analysis of four phenocrysts of plagioclase in the WTHAR with GLO morphology, their compositions fall in the range of andesine to labradorite. The enrichment of anorthite (rim) and Ab (core) in crystal A represents the abnormal crystallization process. Crystal B represents the normal crystallization process with An% content in the core higher than that in the rim (Figure 13d). In phenocrysts C and D the trend of An % content occurs in an oscillatory form (Figure 13 E and F). From the latter, it can be deduced that the phenocrysts crystallized after the recharge of basic magma resulting in the change of the magma chemical composition.

5.1.7. Swallow-tail (ST) and broken crystals (BS)

In some samples, plagioclase crystals with H-shaped outer skeletal envelopes (swallow-tail) are seen, which are not numerous. The frequency of broken crystals in the studied samples (Table 2d, Figure 4b, d, e, and h) indicates that during an explosive eruption, gas-rich vesicles, trapped under high pressure in the plagioclases, escape abruptly from their hosts (Miwa & Geshi, 2012; Renjith, 2014).

5.1.8. Intact crystals (IC)

The intact crystals do not have any micro-texture; however, in the rim of some intact crystals, synneusis textures are observed. The compositional spectrum of plagioclase in this suite ranges from andesine to labradorite and bytownite. In these plagioclases, the amount of An% content decreases from core to rim.

5.2. Magma chamber processes and plumbing model

As mentioned before, various micro-textures were identified in plagioclases of WTHA rocks. The micro-textures are caused by different processes and can be divided into two categories: (i) growth related

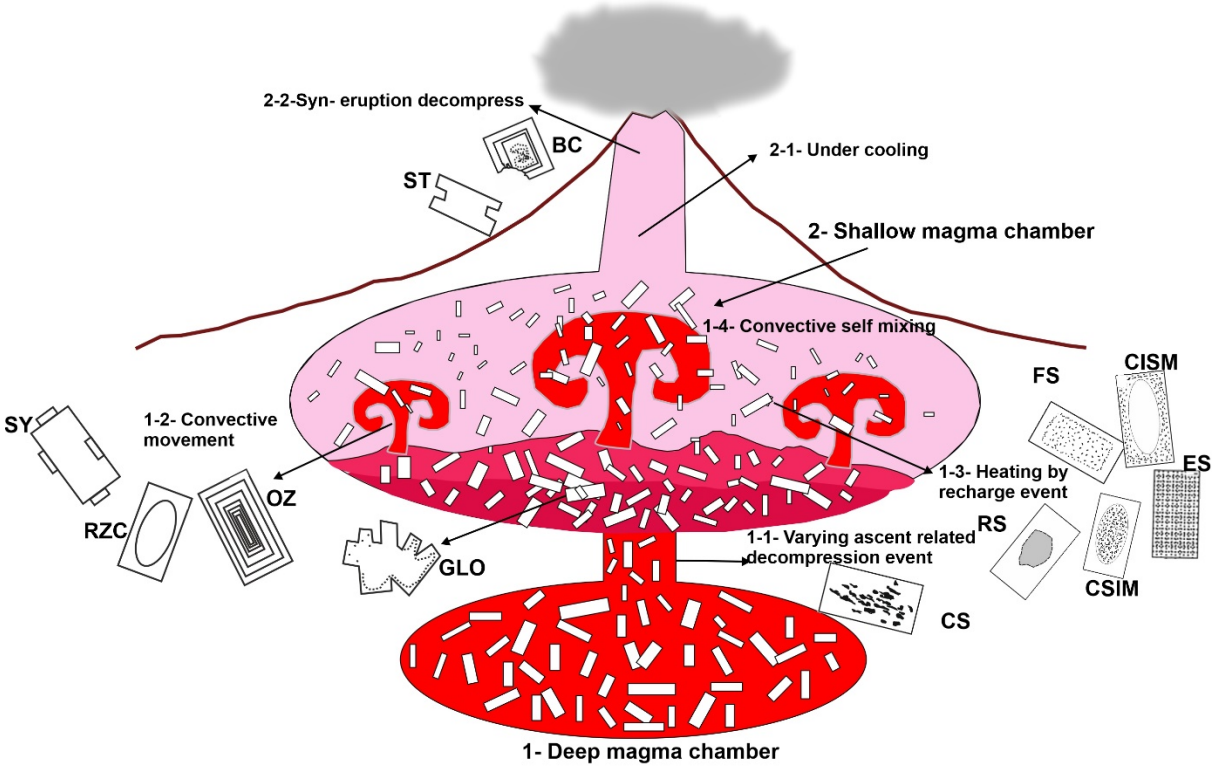

Figure 14. Schematic model of crystallization dynamics and magma plumbing system (modified after Renjith 2014).

textures in the form of coarse-sieved, fine-sieved, core sieved and intact margin, entirely sieved, textures, oscillatory zoning, rounded zone corner and resorption surfaces due to the change in temperature, H_2O content, pressure or composition of the crystallizing melt and results in disequilibrium at the crystal-melt interface; and (ii) morphological textures, such as glomerocrysts, synneusis, swallow-tail crystals and broken crystals, formed by the dynamic behavior of the crystallizing magma such as degassing, eruption and convection. Based on textural observations a simplified magma plumbing model is suggested for the samples studied. In the first stage, hot and silica and volatile saturated magma in the deep magma chamber was crystallizing in a stable magmatic environment. The An-rich intact crystals are produced in this stage. When this crystal-rich magma rises into the upper shallower chamber, the crystals undergo various degrees of dissolution and develop coarse-sieve textures with different shapes and sizes (Figure 4a, c, d, and h). The reason for this variety can be due to the variation in the rate of decompression or H_2O content dissolved in the magma (Renjith, 2014). After the formation of CS micro-textures, some crystals get united as glomerocrysts. The GLO micro-texture that has CS (Figure 4g) indicates that after the development of the CS these crystals aggregatedtogether. This shallow magma chamber was dynamically active by convection or by the input of new magma pulses or a combination of both. As a result, pre-existing and newly brought crystals have further re-grown and developed multiple micro-textures such as fine-sieve, core sieved and intact margin, core intact and sieved margin, entirely sieve, rounded zone corner, oscillatory zoning and resorption surfaces. It is worth noting that the growth of the crystals at this time was constrained by the heterogeneous superheating and convection processes (Viccaro et al., 2012). The frequent presence of FS micro-texture in the crystals can indicate that multiple events of superheating by recharge events have occurred. Crystals with CS micro-texture in their core surrounded by FS and SY micro-textures (Figure 4 a and), indicate that repeated magma processes occurred in the shallow chamber after the formation of CS texture and before the eruption. Recharge brought new pulses of primitive magma which interacted with the pre-existing plagioclases in the shallow chamber causing partial dissolution in the form of FS micro-texture (Renjith, 2014). After partial dissolution process, plagioclases re-equilibrated with the new magma that was rich in Ca and were re-grown as An-rich plagioclase. Based on observed OZ, some plagioclase crystals in the shallow magma chamber have undergone repeated dissolution-regrowth in a convective environment. Another important point to be considered is the temperature changes in the magma chamber. This phenomenon can occur due to self-mixing (recharge of hotter magma at the base of the magma chamber (Couch et al., 2001). During this process, the magma chamber probably has experienced undercooling. Swallow-tail and broken crystal micro-textures are the late stage crystallization products of undercooling-associated syn-eruption or just pre-eruption (Jamshidibadr et al., 2020). Figure 14 shows the schematic model for crystallization dynamics and the magma plumbing system.

6. CONCLUSION

The compositional spectrum of plagioclase phenocrysts in this suite ranges from andesine to labradorite, and even bytownite. Micro-textures and characteristics of these plagioclases reflect the events that took place during crystallizing of these rocks and are as follows: coarse- and fine-sieve textures, oscillatory zoning, resorption surfaces and rounded zone corner, glomerocrysts, synneusis, swallow-tail crystals and broken crystals. These characteristics are due to the changes in temperature, H_2O content or pressure of the crystallizing melt leading to disequilibrium at the crystal-melt interface and effects of the dynamic behavior of the crystallizing magma such as degassing, eruption and convection. The occurrence of these changes can also be related to the self-mixing process in the magma chamber, which combined with a recharge event, can be the reason for the dynamic activities in the magma chamber.

REFERENCES

Alaminia, Z., Karimpour, M.H., Homam, S.M, & Fritz, F., 2013. The Magmatic Record in the Arghash Region (Northeast Iran) and Tectonic Implications. *International Journal of Earth Sciences*, 102:1603–1625.

Alizadeh, E., Ghadami, G., Esmaeily, D., Ma, Ch., Lentz, D, R., Omrani, J., & Golmohammadi, A., 2017. *Origin of 1.8 Ga Zircons in Post Eocene Mafic Dikes in the Roshtkhar Area, NE Iran.* International Geology Review, 60:1855– 1882.

Almasi, A., Karimpour, M.H., Arjmandzadeh, R., Santos, J. F., & Ebrahimi Nasarabadi, Kh., 2019. *Zircon U-Pb Geochronology, Geochemistry, Sr-Nd Isotopic Compositions, and Tectonomagmatic Implications of Nay (NE Iran) Postcollisional Intrusives in the Sabzevar Zone.* Turkish Journal Earth Sciences, 28:372–397.

Baluchi, S., 2019. *Petrology, Geochemistry and Isotope Geology of Jandagh - Arusan Metamorphic- Igneous Complex.* Unpublished Ph.D. Thesis in Geology,

Shahrood University of Technology, Shahrood, Iran (In Persian).

Berberian, F., & King, G.C.P., 1981. *Towards a Paleogeography and Tectonic Evolution of Iran*. Canadian Journal of Earth Sciences, 5: 101-117.

Bennett, E. N., Lissenberg C. G & Cashman K. V., 2019. *The significance of plagioclase textures in mid-ocean ridge basalt (Gakkel Ridge, Arctic Ocean)*. Contributions to Mineralogy and Petrology, 174, 49.

Blundy, J. & Cashman, K., 2005. *Rapid decompression-driven crystallization recorded by melt inclusions from Mount St. Helens Volcano*. Geology, 33 (10), 793e796.

Browne, B.L., Eichelbergera, J.C., Patinob, L.C., Vogelb, T.A., Utoc, K. & Hoshizumi, H., 2006. *Magma mingling as indicated by texture and Sr/Ba ratios of plagioclase phenocrysts from Unzen volcano, SW Japan*. Journal of Volcanology and Geothermal Research, 154, (1e2), 103e116.

Couch, S.R, Sparks, S.J. & Carroll, M.R., 2001. Mineral disequilibrium in lavas explained by convective selfmixing in open magma chambers, Nature, 411, 10371039.

Davidson, J.P., Tepley III, F.J., 1997. Recharge in volcanic systems: evidence from isotope profiles of phenocrysts. Science 275 (5301), 826e829.

Deer, W.A., Howie, R.A., & Zussman, J., 1992. *An Introduction to the Rock forming Minerals*. London, Longman.

Korkmaz, G., & Kurt, H., 2021. *Interpretation of the magma chamber processes with the help of textural stratigraphy of the Plagioclases (Konya-Central Anatolia)*. European Journal of Science and Technology, 25, 222-237.

Ghasemi, H., & Rezaei Kahkhaei, M., 2015. *Petrochemistry and Tectonic Setting of the Davarzan Abbas Abad Eocene Volcanic (DAEV) Rocks, NE Iran.* Journal of Mineralogy and Petrology, 6: 235-252.

Gill, J.B., 1981. *Orogenic Andesites and Plate Tectonics*. Springer, Berlin, 390p.

Ginibre, C., Kronz, A., & Wörner, G., 2002a. High-resolution quantitative imaging of plagioclase composition using accumulated backscattered electron images: new constraints on oscillatory zoning. Contributions to Mineralogy and Petrology 142, 436e448.

Helmy, H.M., Ahmed, A.F., El Mahallawi, M.M. & Ali, S.M., 2004. *Pressure, temperature and oxygen fugacity conditions of calc-alkaline granitoids, Eastern Desert of Egypt, and tectonic implications*. Journal of African Earth. Science. 38, 255-268.

Hoshide T., & Obata M., 2009. *Zoning and resorption of plagioclase in a layered gabbro, as a petrographic indicator of magmatic differentiation*. Earth and Environmental Science Transactions of the Royal Society of Edinburgh, 100, 1–15.

Jamshidibadr M., Tarabi, S., & Gholizadeh K., 2020. *Study of micro-textures and chemistry of feldspar minerals of East Sarbisheh volcanic complex (Eastern Iran), for evidence of magma chamber process*, 12, 10-31.

Kazemi, Z., Ghasemi, H., Tilhac, R., Griffin, W., Shafaii Moghadam, H., O. Re., & Mosivand, F., 2019. *Late Cretaceous Subduction Related Magmatism on the Southern Edge of Sabzevar Basin, NE Iran.* Journal of the Geological Society, 176(3):530. https://doi.org/10.1144/ jgs2018-076

Landi, P., Métrich, N., Bertagnini, A., & Mauro Rosi, M., 2004. *Dynamics of magma mixing and degassing recorded in plagioclase at Stromboli (Aeolian Archipelago, Italy)*. Contributions to Mineralogy and Petrology, 147, 213e227.

Le Bas, M.J., Le Maitre, R.W., Streckeisen, A., & Zanettin, B., 1986. *A chemical classification of volcanic rocks based on the total alkali-silica diagram.* Journal of Petrology, 27, 745-750.

Lindh, A., Kjöllerström, A., & Solyom, Z., 2006. *Localised country-rock contamination and partial homogenisation of a mafic magma: an example from west central Sweden.* Lithos 86: 212–228.

Miwa, T., & Geshi, N., 2012. *Decompression rate of magma at fragmentation: inference from broken crystals in pumice of vulcanian eruption*. Journal of Volcanology and Geothermal Research, 227e228, 76e84.

Mobashergarmi, M., Zaraisahamia, R., Aghazadeh, M., Ahmadikhalaji, A., & Ahmadzadeh, Gh., 2018. *Mineral chemistry and thermobarometry of Eocene alkaline volcanic rocks in SW Germi, NW Iran.* Iranian Journal of Earth Sciences, 10 , 39-51.

Molina, J., Scarrow, J., Montero, P. G., & Bea, F., 2009. *High-Ti amphibole as a petrogenetic indicator of magma chemistry: evidence for mildly alkalic-hybrid melts during evolution of Variscan basic-ultrabasic magmatism of Central Iberia*. Contribution to Mineralogy and Petrology, 158, 69-98.

Nelson S. T., & Montana A., 1992. *Sieve-textured plagioclase in volcanic rocks produced by rapid decompression*. American Mineralogist, 77, 1242-1249.

Pang, K.N., Chung, S.L., Zarrinkoub, M.H., Khatib. M. M., Mohammadi. S., Chiu, H. Y., Chu, Ch. H., Lee, H. Y., Hao, Y., & Lo, Ch. H., 2013. *Eocene–Oligocene post-collisional magmatism in the Lut–Sistan Region, Eastern Iran: Magma Genesis and Tectonic Implications*. Lithos, 180: 234–251.

Pearce, J.A., 1983. *The Role of Sub-Continental Lithosphere in Magma Genesis at Destructive Plate Margins*, Hawksworth, C.J., and Norry, M.J., eds., Continental Basalts and Mantle Xenoliths: Nantwich, Shiva, P. 230–249.

Renjith, ML., 2014. *Micro-textures in plagioclase from 1994e1995 eruption, Barren Island Volcano: Evidence of dynamic magma plumbing system in the Andaman subduction zone*, Geoscience Frontiers 5, 113-126.

Schwindinger, K. R., 1999. *Particle dynamics and aggregation of crystals in a magma chamber with*

application to Kilauea Iki olivines, Journal of Volcanology and Geothermal Research 88, 209 - 238.

Shafaii Moghadam, H., Li, X. H., Ling, X. X., Santos, J. F., Stern, R.J., Li, Q. L.& Ghorbani, Gh., 2015. *Eocene Kashmar granitoids (NE Iran): Petrogenetic constraints from U–Pb zircon geochronology and isotope geochemistry*. Lithos 216–217, 118–135.

Shafaii Moghadam, H., Li, X. H., Stern, R. J., Santoes, J. F., Hgorbani, Gh., & Pourmohsen, M., 2016. *Age and Nature of 560–520 Ma Calc-Alkaline Granitoids of Biarjmand, Northeast Iran: Insights into Cadomian Arc Magmatism in Northern Gondwana.* International Geology Review, 58(12): 1492–1509.

Sepidbar, F., Karsli, O., Palin, R.M., & Casetta, F., 2021. *Cenozoic Temporal Variation of Crustal thickness in the Urumieh-Dokhtar and Alborz Magmatic Belts, Iran.* Lithos, 400-401, 106401. https://doi.org/10.1016/j.lithos.2021.106401.

Shahbazi, H., Sepahi, A.A., & Shakouri, M.A., 2021. *Zircon U–Pb Ages and Petrogenesis of the Middle Eocene Aliabad Daman Pluton, Northeast Iran: Implications for Magmatic Activity Along the Doruneh Fault Zone.* Arabian Journal of Geosciences, 14: 212. https://doi.org/10.1007/s12517-020-06437-w.

Shelley, D., 1993. *Igneous and metamorphic rocks under the microscope*: Chapman and Hall, University Press, Cambridge, Great Britain, 445.

Sivell, W.J. & Waterhouse, J.B., 1988. *Petrogenesis of Gympie Group volcanics: evidence for remnants of an early Permian volcanic arc in eastern Australia*. Lithos, 21, 81-95. http://dx.doi.org/10.1016/0024-4937(88)90012-6.

Sun, S. S. & McDonough, W. F., 1989. *Chemical and isotopic systematics of oceanic of basalts: implication for mantle composition and processes, in: Magmatism in oceanic basins*, edited by: Saunders A. D. and Norry M. J. Geological Society London 42, 313-345.

Tsuchiyama, A., 1985. *Dissolution kenitics of plagioclase in the melt of the system diopside- albite - anorthosite and origin of dusty plagioclase in andesite*. Contributions to Mineralogy and Petrology, 89, 1-16.

Vernon, R. H., 2004. *A practical guide to Rock Microstructure*. Cambridge University Press, Cambridge.

Viccaro, M., Giacomoni, PP, Ferlito C, Cristofolini, R., 2010. *Dynamics of magma supply at Mt. Etna volcano (Southern Italy) as revealed by textural and compositional features of plagioclase phenocrysts*. Lithos, 116, 77-91.

Viccaro, M., Giuffridaa, M., Nicotraa, E. & Ozerov, Y.A., 2012. *Magma storage, ascent and recharge history prior to the 1991 eruption at Avachinsky Volcano, Kamchatka, Russia: inferences on the plumbing system geometry*. Lithos, 140-141, 11-24.

Yan, H., Long, X., Li, J., Wang, Q., Zhao, B., Shu, C., Gou, L. & Zuo, R., 2019. *Arc andesitic rocks derived from partial melts of mélange diaper in subduction zones: Evidence from whole-rock geochemistry and Sr- Nd-Mo isotopes of the Paleogene Linzizong volcanic succession in southern Tibet*. Journal of Geophysical Research: Solid Earth, 124, 456–475. doi.org/10.1029/2018JB016545.

Yousefi, F., Sadeghian, M., Wanhainen, Ch., Ghasemi, H., Papadopoulou,L., Bark, G., Rezaei-Kahkhaei, M. & Koroneos, A., 2017 a . *Mineral chemistry and P-T conditions of the adakitic rocks from Torud–Ahmad Abad magmatic belt, S-SE Shahrood, NE Iran*. Journal of Geochemical Exploration, doi:10.1016/j.gexplo.2017.09.006

Yousefi, F., Sadeghian, M., Wanhainen, Ch., Ghasemi, H. & Frei, D., 2017 b. *Geochemistry, petrogenesis and tectonic setting of middle Eocene hypabyssal rocks of the Torud–Ahmad Abad magmatic belt: An implication for evolution of the northern branch of Neo-Tethys Ocean in Iran. Journal of Geochemical Exploration*. 178, 1–15.

Zhang, L., Li, Sh. & Zhao, O., 2019. *A review of research on adakites*. International geology review 63, 1-18. DOI: 10.1080/00206814.2019.1702592.

Received at: 12. 01. 2023
Revised at: 25. 02. 2023
Accepted for publication at: 11. 03. 2023
Published online at: 02. 05. 2023